

Gas Dynamical Parameters of Detonation Powder Spraying

E. Kadyrov and V. Kadyrov

An investigation is conducted of the gas dynamics of a gas detonation coating process and the mechanism of particle acceleration by the shock wave inside the coating apparatus. Velocities of gas detonation in different gas mixtures are analyzed by applying the conventional hydrodynamic theory of detonation, and the effect of addition gases on the velocity of detonation in oxygen/hydrogen and oxygen/acetylene mixtures is studied. The authors propose a model that allows calculation of particle acceleration and final velocity. This model utilizes the Chapman-Jouquet picture of detonation and assumptions about the linear distribution of the velocity of detonation products behind the front of the detonation wave. The kinetics of particle acceleration by a detonation wave exhibits several novel features and is distinctly different from particle acceleration in other methods of spraying, such as plasma and high-velocity oxyfuel. There is a nonmonotonic dependence of particle velocity upon its coordinate and change in the direction of particle acceleration. Loading distance and total barrel length are important parameters that affect final particle velocity. Results indicate that final particle velocity and, as a consequence, the quality of detonation coatings can be significantly affected by changing the gas mixture composition and the powder loading distance while keeping the remaining operational parameters constant.

1. Introduction

GAS DETONATION coating technology is known to produce coatings of excellent quality for applications in various industries (Ref 1-4). Good design of gas detonation coating apparatus can offer additional benefits, such as economical consumption of gases, cooling water, and electric power, extremely high reliability, and low temperatures of the sprayed substrate. These features make gas detonation coating technology unique and promising for new industrial applications. Knowledge of the fundamental aspects of this technology is limited, however, partly because the phenomenon of gas detonation and its propagation represents a strongly nonequilibrium process on a millisecond scale. This complicates the study of the kinetics and thermodynamics of the interaction between the particle and the detonation wave on both a theoretical and an experimental level.

This paper investigates theoretically the gas dynamics of the detonation process in several gas compositions and the interaction between a particle and a detonation wave inside detonation spraying apparatus. Better understanding of the gas dynamics of the complex detonation spraying process and interactions in two-phase flow will provide a means of better control. This in turn will expand the capabilities and applications of gas detonation coating technology.

2. Gas Detonation Coating Apparatus

Gas detonation equipment was originally developed and patented in the United States by Union Carbide Corporation in

Keywords: Chapman-Jouquet point, gas detonation, reaction front, shock wave

E. Kadyrov, Materials Science Program, University of Wisconsin—Madison, Madison, WI 53706, USA; **V. Kadyrov**, Institute for Materials Science, Kiev 252142, Ukraine

1955 (Ref 5) and independently in 1969 at the Institute of Materials Science (Kiev, Ukraine) (Ref 6, 7). Since then, detonation coating of various materials has been applied in various industries (mostly aircraft) (Ref 8) in the United States, Japan, and the former Soviet Union. However, gas detonation coating equipment generally has been unavailable for broad use in industry and research laboratories.

A typical gas detonation coating process consists of the following stages. A portion of a flammable gas mixture (oxygen and acetylene, for example) is fed through a mixer into a tubular barrel closed at one end. Simultaneously, a powder of the sprayed material is injected through a powder feeder before the explosion is triggered by a spark plug. Combustion of the gas mixture leads to a detonation effect and formation of a high-pressure ultrasonic wave, which propagates the hot gas stream and accelerates the powder particles. The resulting powder particle velocity can be as high as 1200 m/s (Ref 8). Collision of the powder with the substrate forms a high-density coating with strong adhesion. After the spraying cycle is finished, the powder and the fuel are injected again, and the process repeats. Depending on the type of spray material, detonation gas spraying units can repeat the process at rates of up to 10 runs per second.

The geometry of the detonation chamber must allow a steady detonation, which also depends on the mixture composition, temperature, and pressure. The detonation wave tends to propagate in all directions, including into the gas supply, creating an explosion hazard. This effect is called backfiring and must be considered in the design of gas detonation equipment. The typical solution to this problem is to use an inert gas (e.g., nitrogen) in order to separate different portions of the fuel from one another and to prevent propagation of the detonation wave into the gas distributor (Ref 3). A cyclic gas diagram of the process incorporating this solution is shown in Fig. 1. The process consists of four stages: (1) injection of the oxygen and fuel mixture into the combustion chamber, (2) injection of the powder and nitrogen, which separates the gas supply from the explosion area and prevents backfiring, (3) ignition of the mixture and powder ac-

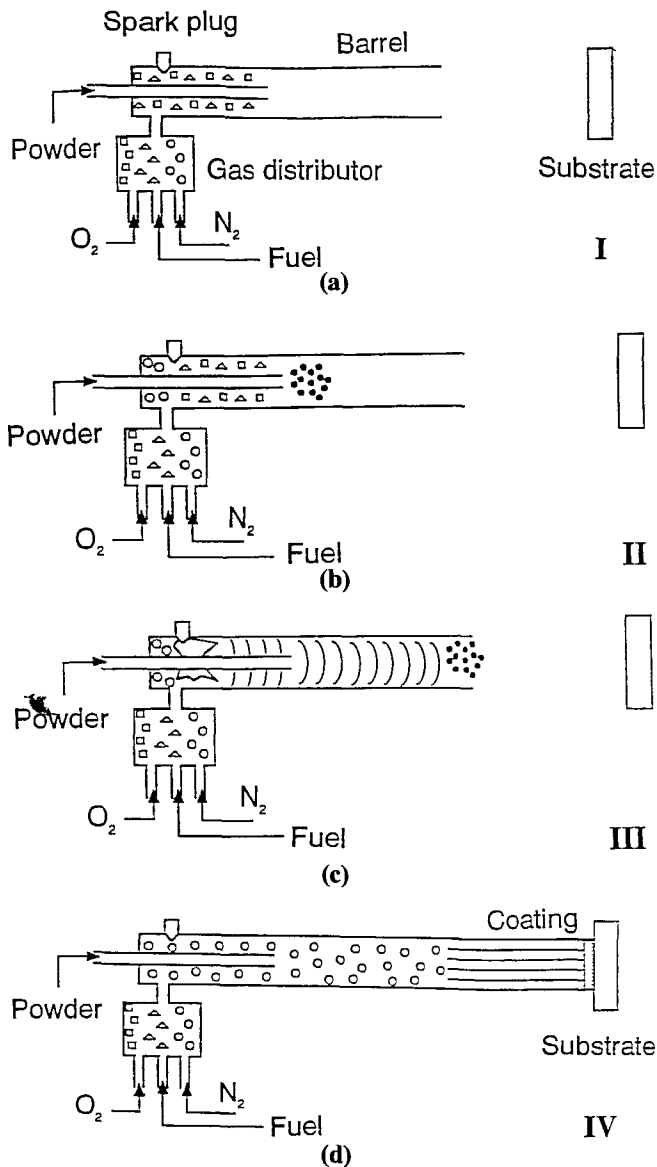


Fig. 1 Cycle gas diagram of the detonation process, using nitrogen as a buffer gas. (a) Injection of fuel and oxygen into combustion chamber. (b) Injection of powder and nitrogen gas. (c) Gas detonation and powder acceleration. (d) Chamber ventilation

celeration by the detonation wave, and (4) ventilation of the barrel by nitrogen gas. After the barrel is purged by nitrogen, the apparatus is ready for the next cycle, and the process starts over. Thus, the gas detonation coating process is intermittent in nature, which allows the temperature of the sprayed substrate to be kept low and undesirable thermal deformations of the substrate to be avoided.

The substrate temperature typically stays below 100 °C, and additional cooling makes it possible to bring it down to room temperature. This enables spraying onto low-melting-point materials and precision parts without inducing thermal deformation. Operations of this process without the use of high-pressure gas and water lines and without a Laval nozzle inside the barrel becomes very simple and economical. Typical gas pressures are

20 to 30 psi, and consumption of gas per unit mass of sprayed material is typically four to eight times less than for high-velocity oxyfuel (HVOF) spraying. On the other hand, high particle velocity and the effect of hot pressing (Ref 8) when the detonation waves collide with the substrate produce excellent quality coatings with low porosity (0 to 2%) and high adhesion (up to 250 MPa). The final coating properties and microstructure depend on numerous parameters, such as type of sprayed material, gas mixture composition, firing frequency, and detonation gun geometry.

The use of nitrogen as a buffer gas in a detonation process requires a rather complicated gas supply system with mechanically moving valves (Ref 6), which reduces the reliability of the apparatus and, more importantly, limits the firing frequency to eight shots per second. Greater firing frequency is beneficial since it increases the overall productivity of the apparatus and enhances the efficiency of powder use. After the apparatus is purged by nitrogen, some amount of gas is left inside and mixes with a new portion of fuel and oxygen injected into the combustion chamber. This effect changes the properties of the detonation wave, particularly its velocity, and degrades the quality of the coatings. This effect is considered in more detail in the next section.

3. Properties of the Detonation Wave

The effect of detonation in gases and the properties of the detonation wave have been studied in detail by Bertlo and Le Châtelier in the late 19th century and later by other researchers, including Chapman, Jouquet, Semenov, and Zeldovitch (Ref 9). Experimental studies have established that:

- The velocity of the detonation wave varies between 1000 and 3000 m/s, depending on the composition of the gas mixture, which is several times higher than the speed of sound in these mixtures at normal conditions.
- The velocity of the detonation is almost completely independent of the barrel material, the thickness of its walls, and its diameter, provided that it exceeds the critical diameter.
- The velocity of the detonation does not depend on the conditions behind the detonation wave; that is, it matters not whether the ignition occurs at the open end of the barrel or at the closed end.
- The velocity of the detonation weakly depends on the temperature of gas mixture.
- Increased pressure (density) of the gas mixture increases the velocity of the detonation wave; this increase is small at low pressures and becomes larger at higher pressures.
- Each gas mixture has an optimal composition that corresponds to the maximum speed of the detonation wave.

Qualitatively, parameters of the detonation wave (velocity, pressure, density, temperature, energy) in different gas mixtures can be obtained by using the phenomenological hydrodynamical theory of detonation (Ref 9). According to this theory, propagation of the detonation is caused by propagation of a shock wave in the combustible mixture. If the amplitude of this wave exceeds a certain value, the wave is capable of inducing intensive chemical reaction beyond its front, which supplies energy to the detonation process and keeps its parameters stationary.

Table 1 Parameters of the detonation wave in a hydrogen/oxygen mixture with addition of various gases

Fuel mixture	p_1/p_0	T_1, K	$D, m/s$
$2H_2 + O_2$	18.0	3583	2806
$(2H_2 + O_2) + O_2$	17.4	3390	2302
$(2H_2 + O_2) + 4H_2$	16.0	2976	3627
$(2H_2 + O_2) + N_2$	17.4	3367	2378
$(2H_2 + O_2) + 3N_2$	15.6	3003	2033
$(2H_2 + O_2) + 1.5Ar$	17.6	3412	2117

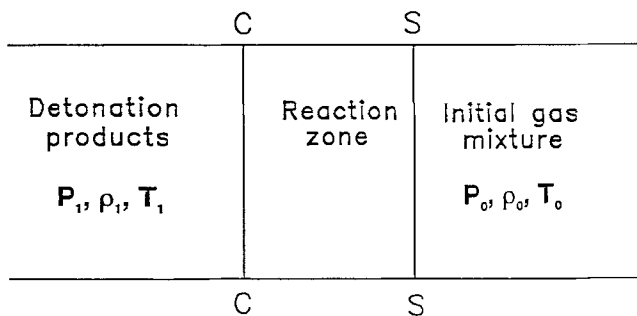


Fig. 2 Structure of the detonation wave. SS, Chapman-Jouquet surface; CC, detonation wave front

Thus, propagation of detonation includes motion of the shock wave, a zone of chemical reaction, and final products of detonation (Fig. 2). The surface separating the zone of chemical reaction and the detonation products is called a Chapman-Jouquet surface (C-C). The parameters of the detonation products at this surface are called detonation wave parameters. The initial gas mixture is separated from the zone of chemical reaction by the front of the shock wave (S-S). The following notation will be used: D , speed of the detonation; u_1 , velocity of the detonation products behind the wave front; p_1 , ρ_1 , and T_1 , pressure, density, and temperature, respectively, of the detonation products at the Chapman-Jouquet surface; p_0 , ρ_0 , and T_0 , the same parameters before the zone of chemical reaction; and Q_0 , specific energy of chemical reaction during the detonation. At the Chapman-Jouquet surface, the velocity of detonation is equal to the speed of excitation propagation in the detonation products (with respect to a motionless observer):

$$D = u_1 + v_0 \quad (\text{Eq 1})$$

where v_0 is the local speed of sound for the detonation products (corresponding to their state). Hydrodynamic theory gives the following expressions for parameters of the detonation wave. The velocity of the detonation wave is expressed as (Ref 9):

$$D = \sqrt{2(k^2 - 1)Q_0} \quad (\text{Eq 2})$$

where $k = c_p/c_v$, and c_p and c_v are the specific heat of the detonation products at constant pressure and volume, respectively. Temperature and pressure of the detonation products are given by:

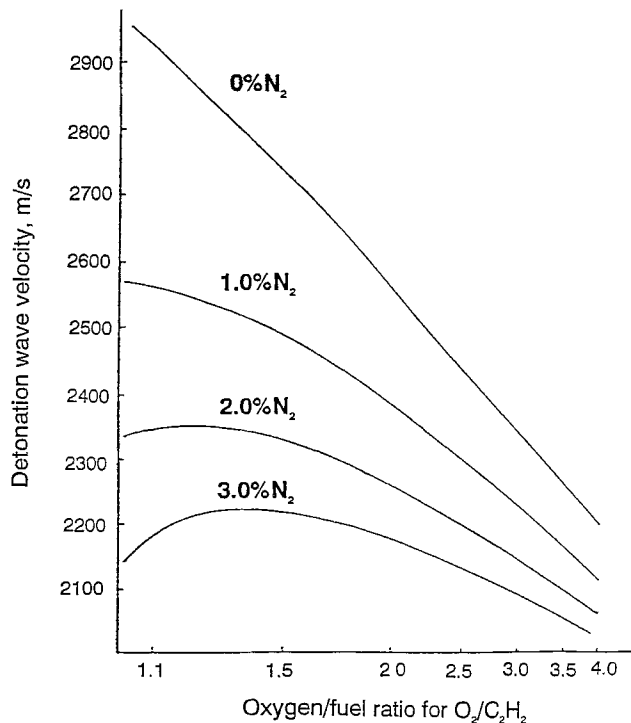


Fig. 3 Effect of nitrogen gas on the detonation speed in oxygen/acetylene mixture

$$T_1 = \frac{2k}{k+1} \frac{Q_0}{C_v} \quad (\text{Eq 3})$$

$$p_1 = 2(k-1)\rho_0 Q_0 \quad (\text{Eq 4})$$

Alternatively, the velocity of the detonation wave can be found from:

$$D = \frac{k+1}{k} \sqrt{\frac{8310k}{\mu_1} T_1} \quad (\text{Eq 5})$$

where μ_1 is the average molecular weight of the detonation product. It can be seen that every parameter of the detonation is very sensitive to the composition of the combustible fuel as well as to the fuel/oxygen ratio. The possibility of changing the properties of the detonation wave over a broad range by changing the composition of the combustible mixture and keeping the pressure and the temperature of the mixture constant is an important feature of gas detonation coating technology.

Equations 3 to 5 were used to calculate parameters of the detonation wave for various gas mixtures. Table 1 shows the results of calculation of detonation parameters for the hydrogen/oxygen mixture with different additions. Addition of helium to a pure hydrogen/oxygen mixture increases the detonation speed, but addition of argon decreases the speed, while the temperature remains about the same for both cases. Generally, addition of light gases will increase the detonation speed, and addition of heavier gases will decrease the speed. Velocity of detonation in an oxygen/hydrogen mixture can be as high as 3627 m/s for a mixture with an excess of hydrogen and as low as

4. Analysis of Basic Interactions and Computational Model

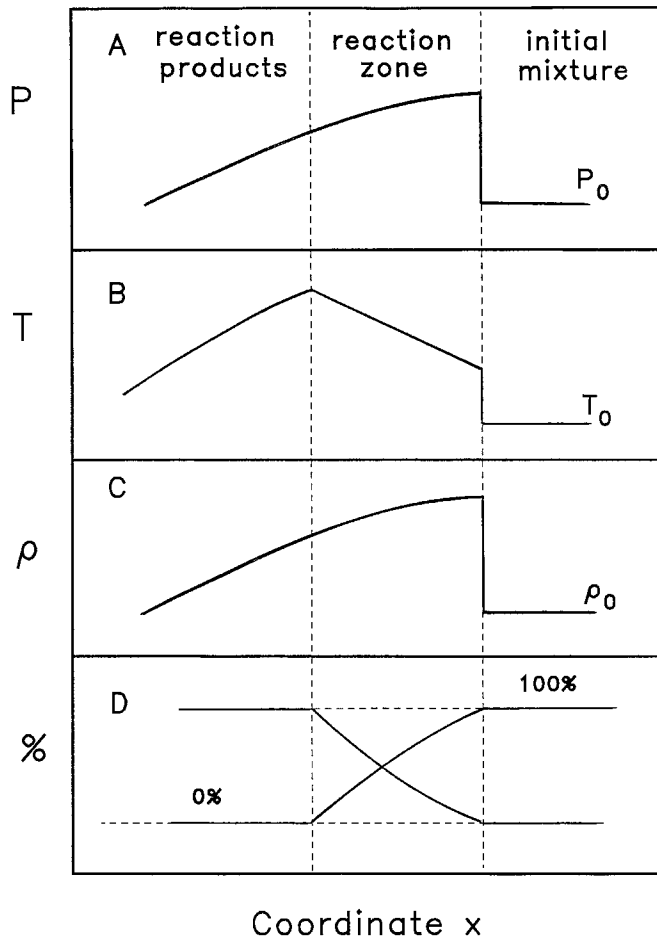


Fig. 4 Qualitative picture of pressure (a), temperature (b), density (c), and concentration (d) distributions in the detonation wave

2112 m/s for a ternary mixture with added argon. Thus, velocity of detonation can be changed over a broad range by addition of various gases at constant initial temperature and pressure, which represents an additional technological benefit of this process.

Figure 3 shows the results of a similar calculation for an oxygen/acetylene mixture with a different concentration of nitrogen. This case corresponds to a mixture frequently used in industrial equipment. It is seen that for a pure oxygen/acetylene mixture, the velocity of detonation increases with an increased amount of acetylene. However, in the presence of several percent of nitrogen, a maximum develops in the velocity dependence, and the optimal composition of the mixture now depends on the amount of nitrogen present. It is important to note that the velocity of detonation reduces sharply with increased content of nitrogen in the mixture. For example, 3% N can reduce the speed of detonation by 600 to 800 m/s. This effect results in lower accelerated particle speeds and degraded coating quality. Use of other gases, such as helium, is not beneficial in terms of economy.

After the initial ignition, the gas combustion propagates in all directions and, after some distance, transforms into a steady detonation wave characterized by very stable parameters of speed, pressure, temperature, and density gradients. The front of the detonation wave and the reaction zone are followed by detonation products that are characterized by their own temperature, density, speed, and chemical composition. However, it is important to note that at any given point inside the barrel, the velocity $u(x,t)$, temperature $t(x,t)$, pressure $p(x,t)$, and density $\rho(x,t)$ of gas detonation products are now functions of coordinate and time, whereas in other methods of spraying, such as HVOF, a stationary picture of combustion can be utilized that is completely independent of time.

One can image propagation of the detonation wave as a stationary distribution of density, temperature, pressure, and velocity moving with some speed distribution. This qualitative picture is shown in Fig. 4. At the leading edge of the detonation wave, the temperature increases dramatically. Behind the front, the temperature rises gradually in the reaction zone and then decreases gradually with increasing distance from the wave front. There are also steplike increases in pressure and density at the detonation wave front, which then gradually decrease behind it. Initial chemical composition of the mixture changes to the composition of the reaction products while passing through the reaction zone. It is assumed that the reaction zone has an infinitely small thickness and that the zone of the reaction products is separated from the initial gas mixture by the detonation wave front. The detonation wave front propagates to the right with velocity D , which is given by Eq 1 to 5. The detonation products have a lesser velocity, which depends on the distance from the wave front.

Consider the interaction of a particle with the detonation wave and the detonation products that follow. In this analysis, particles are assumed to be spherical, and all interparticle interactions are neglected. We assume a one-dimensional picture of motion parallel to the detonation gun barrel and do not take into account any forces perpendicular to this direction. For example, gravity and buoyancy forces that act in the direction perpendicular to the direction of motion are not considered in calculating the acceleration. Particle acceleration is caused by simultaneous action of the following forces. When the detonation wave front passes through the particle, it experiences a force related to the pressure jump in the wave front. This force can be estimated as:

$$F_p = \frac{\pi d_p^2}{4} \Delta p \quad (\text{Eq 6})$$

where d_p is the diameter of the particle and Δp is the pressure jump across the detonation wave front. This force reaches a maximum when the detonation wave front passes through the central particle cross section and decreases as the particle separates from the front. Large temperature gradients, ∇T , in the flow cause another force:

$$F_t = -k \frac{\mu_g d_p \nabla T}{2\rho_g T} \quad (\text{Eq 7})$$

Table 2 Forces acting on the particle in the detonation wave

Particle type	F_p, N	F_t, N	F_g, N
Al_2O_3	6.2×10^{-4}	1.85×10^{-13}	3.16×10^{-4}
Tungsten	6.2×10^{-4}	0.71×10^{-13}	3.16×10^{-4}

where $k = 9\pi\lambda_g/(2\lambda_g + \lambda_p)$; λ_g and λ_p are coefficients of heat conduction for gas and particle, respectively; μ_g is gas viscosity; T is gas temperature; and ρ_g is gas density. Due to intensive cooling in the vicinity of barrel walls, a transverse temperature gradient that can be substantial (10^4 °C/m) also exists. This effect is neglected in our calculations. After the particle exits the wave front, it interacts with the products of detonation and experiences a drag force due to a difference in their respective velocities. This force can be expressed as (Ref 10):

$$F_g = \frac{3}{4} c_d \left[\frac{m_p \rho_g}{\rho_p} \right] \left[\frac{u-v}{d} \right]^2 \quad (\text{Eq 8})$$

where c_d is the drag coefficient, ρ_p is particle density, and v is particle velocity. The drag induced on the particle in this supersonic flow was calculated using the empirical correlation of Walsh (Ref 11) and is valid up to mach 2. The drag coefficient for single particles was used, and interaction between the particles was neglected. The drag coefficient calculated from this relation is only several percent higher than the drag coefficient evaluated from the well-known correlation at low velocities (Ref 12):

$$c_d = \frac{24}{Re} (1 + 0.15Re^{0.687}) \quad (\text{Eq 9})$$

where Re is a Reynolds number. This expression gives good prediction (Ref 11) for experimental data up to $Re = 200$. The drag force reaches a maximum immediately after the particle enters the detonation products and gradually reduces as the particle accelerates and the detonation products slow.

Using Eq 6 to 9, we can estimate these forces and compare them. The estimate was performed for particles of aluminum oxide (Al_2O_3) and tungsten having diameters of 20 μm with $\lambda_p = 31.9$ and 76.5 $\text{W/m} \cdot \text{K}$, respectively. The following values were used in this estimate: $u = 1900$ m/s , $\rho_g = 2.431$ kg/m^3 , $\rho_p = 19,290$ kg/m^3 for tungsten and 3980 kg/m^3 for Al_2O_3 , $v = 0$ m/s , $\mu_g = 8 \times 10^{-5}$ $\text{N} \cdot \text{s/m}^2$, $\nabla T = 10^5$ K/m , and $\Delta p = 10^6$ N/m^2 . Results of this calculation are presented in Table 2. As can be seen, the force due to the pressure jump in the wave front F_p has the same order of magnitude as the drag force F_g . For an Al_2O_3 particle, $F_p = 6.15 \times 10^{-4}$ N and $F_g = 3.21 \times 10^{-4}$ N . At the same time, the force due to the temperature gradient is seven orders of magnitude smaller and can be neglected in calculations. Although forces F_p and F_g can both result in a large particle acceleration, the time of their action is very different. Force F_p acts upon the particle during a much shorter time when the particle passes through the detonation wave front. Assuming that the pressure jump occurs in a very narrow zone (Fig. 4), this time can be estimated as $t_0 = d_p/D$ and is on the order of nanoseconds. During this time the velocity of the particle will be changed by:

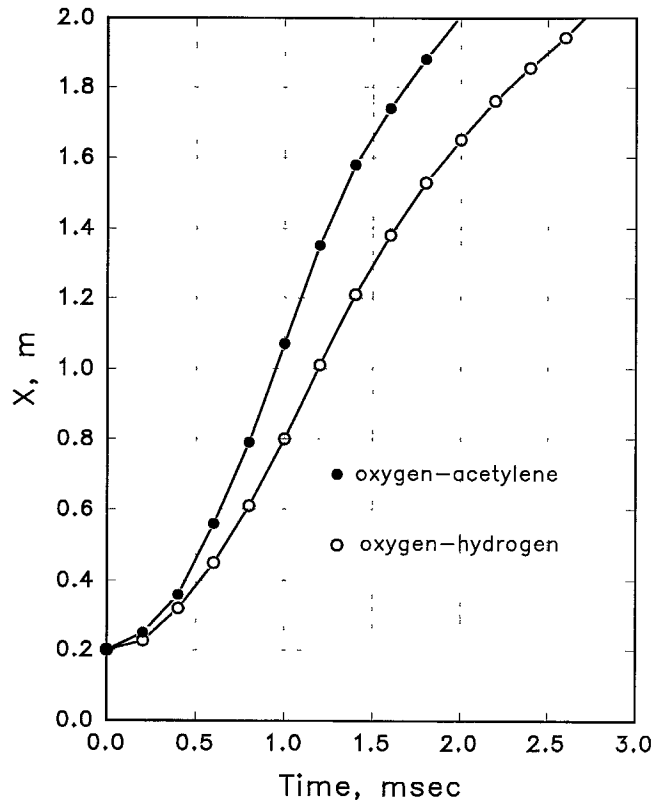


Fig. 5 Coordinate of 20 μm Al_2O_3 particle versus time for oxygen/acetylene and oxygen/hydrogen stoichiometric mixtures

$$\Delta v = \frac{3\Delta p}{2\rho_p D} \quad (\text{Eq 10})$$

Estimates from Eq 10 show that passing through the detonation wave front will increase the speed of Al_2O_3 particles by 0.257 m/s and that of tungsten particles by 0.043 m/s . These values are much smaller than the final particle speed, which is on the order of 1000 m/s . Thus, because of the short period of particle interaction with the front of the detonation wave, its effect on particle speed is insignificant and can be ignored. The major contribution to acceleration is interaction between the particle and the products of detonation, which occurs for a much longer period on the order of milliseconds. Particle acceleration during the initial stage of motion is very large and can be estimated from Eq 8. For an Al_2O_3 particle, the acceleration is equal to 2.08×10^7 m/s^2 ; for a tungsten particle, 3.97×10^6 m/s^2 . Based on these results, the equation of motion for the particle can be written as:

$$m_p \frac{dv}{dt} = F_g \quad (\text{Eq 11})$$

where F_g is given by Eq 8. It is important to note, however, that the velocity and density of the detonation products are not constant and depend strongly on the distance between the particle and the detonation wave front. If the effects of friction between gas and the gun barrel and the effects of particles on the gas are neglected, then analytical solutions for velocity, density and

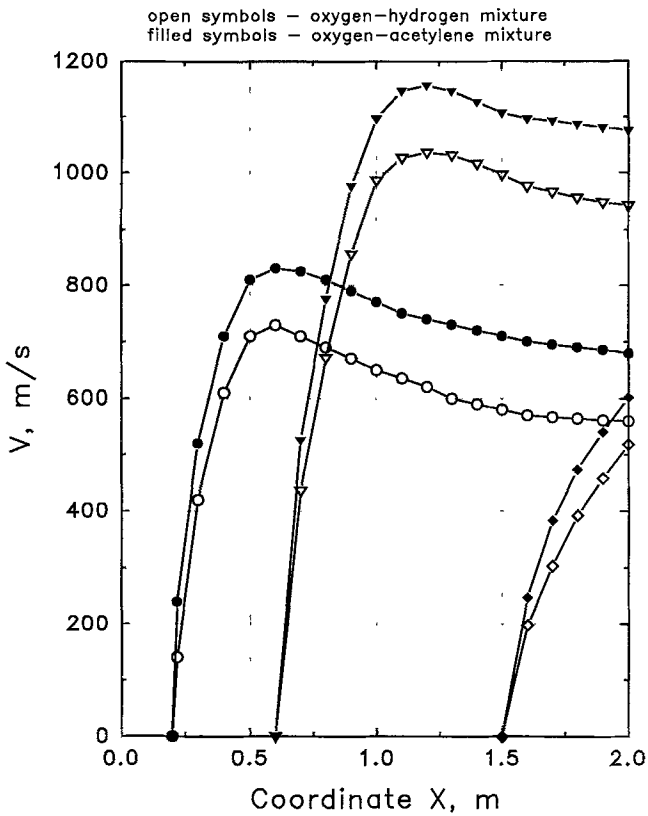


Fig. 6 Velocity of 20 μm Al_2O_3 particle versus particle coordinate for oxygen/acetylene and oxygen/hydrogen stoichiometric mixtures

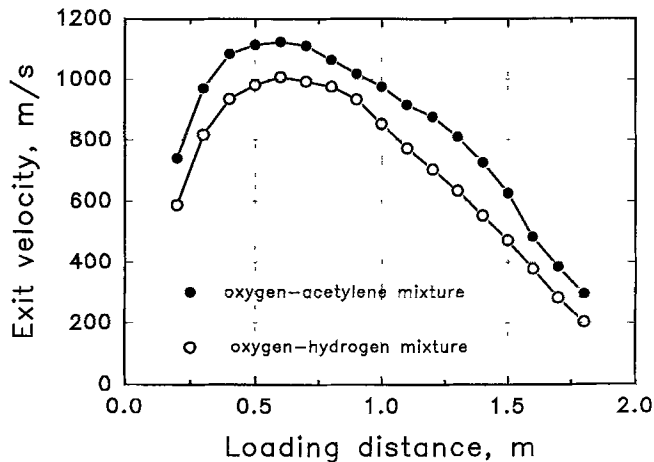


Fig. 7 Exit velocity of 30 μm Al_2O_3 particle versus loading distance for oxygen/acetylene and oxygen/hydrogen stoichiometric mixtures

pressure distributions in the detonation wave exist (Ref. 13). In our model we use the following expressions, which were developed in Ref. 13 and based on analysis of equations of adiabatic gas expansion:

$$u = u_1 \left(2 \frac{x_f - d}{x_f} - 1 \right) \quad (\text{Eq 12})$$

$$\rho = \rho_x + \rho_1 \left(2 \frac{x_f - d}{x_f} - 1 \right) \quad (\text{Eq 13})$$

where x_f is the coordinate of the detonation wave front, d is the distance between the particle and the detonation wave front, and ρ_x is the density of the detonation products at point $x = x_f/2$. Equation 11 was integrated numerically by using MATLAB (Matlab, Inc., Asheboro, NC) software with the standard fourth-order Runge-Kutta-Fehlberg method. The accuracy of the obtained solution was estimated to be 1%. The calculations were performed for Al_2O_3 particles with diameters of 20 and 30 μm . Two different gas mixtures were considered: stoichiometric oxygen/acetylene and oxygen/hydrogen with D values of 2820 and 2363 m/s, respectively. Results of these calculations are presented in Fig. 5 to 7 and discussed in the next section.

5. Results and Discussion

Figure 5 shows the position of a 20 μm particle versus time for oxygen/acetylene and oxygen/hydrogen gas mixtures. Acceleration in an oxygen/acetylene mixture is faster due to the higher speed of the detonation wave. It takes the particle 2.0 ms to exit the detonation gun barrel for the oxygen/acetylene mixture and 2.7 ms for the oxygen/hydrogen mixture. An interesting feature of the $x(t)$ graph is that it changes the sign of its curvature (downward to upward) at an approximate time of 1.4 ms, indicating a change in particle acceleration direction. This point is further illustrated by results plotted in Fig. 6, which shows the velocity of 20 μm particles as a function of particle position inside the detonation gun barrel for different loading distances and gas mixtures. The loading distance is defined as the distance from the point where the detonation wave is initiated to the point where the particle is injected into the barrel.

These results exhibit several striking features. First, the acceleration of the particle from zero to a maximum speed occurs in a small interval on the order of 20 to 40 cm during approximately 0.1 to 0.2 ms. This can be explained in terms of initial particle acceleration by a high-speed gas flow following the detonation wave front. As the detonation wave propagates forward and the particle separates from the wave front, the velocity of the detonation products reduces and, at some point, becomes smaller than the particle speed. At this moment the drag force changes its direction, and the particle starts to slow down. This effect results in a well-defined peak in the velocity curve, after which it slowly reduces its magnitude. This dependence of particle velocity on its coordinate is distinctly different from particle acceleration dependence in other spraying apparatus, such as HVOF. In HVOF spraying, the velocity of the particle while inside the HVOF jet is a monotonically increasing function of its coordinate and, in the infinite time limit, approaches the velocity of the stream (Ref 14).

Another important result is that both the maximum and the final particle velocities depend strongly on particle loading distance. By the loading distance we define the distance between the point of detonation wave creation to the point of particles injection. For example, for a loading distance of 20 cm with an oxygen/acetylene mixture, particle velocity reaches a maximum of 837 m/s, while for a loading distance of 60 cm, the corre-

sponding number is 1152 m/s. This is due to the longer acceleration path for the particle; the distance between the detonation wave front and the zero-velocity point in the gas increases as the wave propagates inside the barrel. From this point of view, it is beneficial to increase the loading distance. However, this increase eventually reduces the total path of the particle inside the barrel and limits its velocity. This point is illustrated by data for a 150 cm loading distance, at which the particle does not reach its maximum speed. Competition between these two effects defines the optimum loading distance. Final particle speed for 30 μm particles versus loading distance is plotted in Fig. 7, which shows that the final particle speed has a clear maximum at loading distances of 40 to 60 cm. In general, the position of the maximum depends on several parameters, such as type of gas mixture, particle size and material, and barrel length. Hence, the optimum loading distance must be calculated for each particular case. In HVOF, reducing the loading distance (distance from the beginning of accelerating channel to the point of particle injection) causes an increase in accelerating path and the final particle speed.

6. Conclusions

The velocity of gas detonation propagation for an oxygen/acetylene mixture with added nitrogen and for an oxygen/hydrogen mixture with various addition gases is calculated using equations based on the phenomenological hydrodynamic theory of detonation in gases. The velocity of gas detonation depends strongly on the composition of the combustible mixture and can be increased in many cases by additions of light gases. Analysis of basic interactions between the particle and the detonation wave reveals the major contributor to acceleration to be the interaction with the detonation products; the thermal gradient force and interaction with the detonation wave front, on the other hand, can be ignored. Linearly decreasing velocity of the detonation products gives rise to a very peculiar mechanism of particle acceleration that is distinctly different from particle acceleration in HVOF and flame spraying. Acceleration of the particle changes direction while the particle is still inside the barrel, and the velocity of the particle has a nonmonotonic dependence on its coordinate. Exit particle speed can be strongly affected by loading distance and total barrel length—important parameters that influence the detonation coating quality. The optimal loading distance must be calculated for each particular detonation gun geometry, combustible mixture composition, and particle size and material.

Although our approach yields a basic understanding of the problem and a number of practical parameters, the results obtained should be used with some caution because they involve

many approximations. For example, we have used simple linear expressions for the speed of detonation products behind the detonation wave front and have completely neglected effects of particles on the properties of the detonation wave. More precise formulation of the problem, including writing the fundamental equations of momentum, mass, and energy conservation for gas and solid phases, is needed. Such calculations—combined with experimental research—represent a future challenge and will deepen the understanding of this technology.

References

1. M.L. Thorpe and H.J. Richter, A Pragmatic Analysis and Comparison of HVOF Processes, *J. Therm. Spray Technol.*, Vol 1 (No. 2), 1992, p 161-170
2. P. Vuoristo, K. Niemi, and T. Mantyla, Hard Oxide Coatings Deposited by Plasma and Detonation Gun Spraying Techniques, *Proc. 2nd Plasma-Technik-Symp.*, S. Blum-Sandmeier, H. Eschnauer, P. Huber, and A.R. Nicoll, Ed., Plasma-Technik Ag, Wohlen, Switzerland, 1991, p 311-322
3. P. Vuoristo, K. Niemi, and T. Mantyla, On the Properties of Detonation Gun Sprayed and Plasma Sprayed Ceramic Coatings, *Thermal Spray: International Advances in Coating Technology*, C.C. Berndt, Ed., ASM International, 1992, p 171-175
4. K. Niemi, P. Vuoristo, and T. Mantyla, Properties of Alumina-Based Coatings Deposited by Plasma Spray and Detonation Gun Spray Processes, *J. Therm. Spray Technol.*, Vol 3 (No. 2), 1994, p 199-203
5. R.M. Poorman, H.B. Sargent, and R. Lamprey, Method and Apparatus Utilizing Detonation Waves for Spraying and Other Purposes, U.S. Patent 2,714,563, 1955
6. V.A. Nevgod, V.H. Kadyrov, and A. Khairutdinov, Gas Detonation Apparatus, U.S. Patent 4,687,135, 1987
7. V.A. Nevgod, V.H. Kadyrov, and A. Khairutdinov, Gas Detonation Apparatus, U.S. Patent 4,669,658, 1987
8. V. Kadyrov, Detonation Coating Technology, *J. Jpn. Therm. Spray Soc.*, Vol 29 (No. 4), 1992, p 14-25
9. Y.B. Zeldovitch and A. Kompaneets, *Theory of Detonation*, Gostechizdat, Moscow, 1955 (in Russian)
10. R.I. Nigmatulin, *Dynamics of Many-Phase Media*, Nauka, Moscow, 1987, p 464 (in Russian)
11. M.J. Walsh, Drag Coefficient Equations for Small Particles in High Speed Flows, *Am. Inst. Aeronaut. Astronaut. J.*, Vol 13 (No. 11), 1975, p 1526-1528
12. L.B. Torobin and W.H. Gauvin, Fundamental Aspects of Solids-Gas Flow, Part I: Introductory Concepts and Idealized Sphere Motion in Viscous Regime, *Can. J. Chem. Eng.*, Vol 37, 1959, p 129-141
13. E.S. Schetnikov, *Physics of Gas Combustion*, Nauka, Moscow, 1965, p 97 (in Russian)
14. W.L. Oberkampf and M. Talpallikar, Analysis of a High Velocity Oxygen Fuel (HVOF) Thermal Spray Torch. Part 2: Computational Results, *Thermal Spray Industrial Applications*, C.C. Berndt and S. Sampath, Ed., ASM International, 1994, p 387-392